Removal of Indigo Carmine by a Ni Nanoscale Oxides/Schoenoplectus acutus Composite in Batch and Fixed Bed Column Systems

S. Sánchez-Rodríguez[a], J. Trujillo-Reyes[a], E. Gutiérrez-Segura[a], M. Solache-Ríos[b] & A. Colín-Cruz[a]

[a] Facultad de Química, Universidad Autónoma del Estado de México, Toluca, Estado de México, México

[b] Departamento de Química, Instituto Nacional de Investigaciones Nucleares, Delegación Miguel Hidalgo, México, D.F., México
Accepted author version posted online: 19 Feb 2015.

Click for updates

PLEASE SCROLL DOWN FOR ARTICLE

Taylor & Francis
Taylor & Francis Group

Removal of Indigo Carmine by a Ni Nanoscale Oxides/*Schoenoplectus acutus* Composite in Batch and Fixed Bed Column Systems

S. Sánchez-Rodríguez,[1] J. Trujillo-Reyes,[1] E. Gutiérrez-Segura,[1] M. Solache-Ríos,[2] and A. Colín-Cruz[1]

[1]*Facultad de Química,Universidad Autónoma del Estado de México, Toluca, Estado de México, México*
[2]*Departamento de Química, Instituto Nacional de Investigaciones Nucleares, Delegación Miguel Hidalgo, México, D.F., México*

Removal behavior of indigo carmine by *Schoenoplectus acutus* and Ni nanoscale oxides/*Schoenoplectus acutus* composite was determined. The characterization of both materials was done by TEM, SEM/EDS, DRX, and BET. Experimental data were best fitted to pseudo second order and Langmuir-Freundlich models for kinetics and isotherm, respectively; these results indicate a chemisorption mechanism on heterogeneous materials. Adsorption capacity of Ni nanoscale oxides/Schoenoplectus acutus composite was high in comparison with other adsorbents (760 mg/g). Adsorption of dye is not affected by pH (3 to 9). Metal nanoparticles supported on cheap and eco-friendly adsorbents are an alternative for the removal of dyes from wastewater.

INTRODUCTION

Dyes are pollutants which are generally present in aqueous effluents of the textile, leather, food processing, dyeing, cosmetics, paper, and dye manufacturing industries. They are synthetic aromatic compounds with various functional groups. The worldwide high level of production and extensive use of dyes generate wastewaters which causes environmental pollution (1).

Wastewaters containing dyes are very difficult to treat because they are recalcitrant molecules (particularly azo dyes), resistant to aerobic digestion, biologically non-degradable, and stable to oxidizing agents. Common methods for removing dyestuffs are economically unfavorable and/or technically complicated. Many methods for treating dyes in wastewater have not been applied at a large scale (2) because of their high costs associated with their practical applications to remove trace amounts of impurities.

Among several chemical and physical methods, adsorption process is one of the effective techniques that has been successfully employed for the removal of low concentrations of dyes from aqueous media. Activated carbon is regarded as an effective but expensive adsorbent due to its high costs of manufacturing and regeneration. Some adsorbent materials including peat (3), chitin (4), silica (5), perlite (6), and some agricultural wastes have been tested to reduce dye concentrations from aqueous solutions (7). The adsorption capacities of the above-mentioned adsorbents are not very high. In order to improve the efficiencies of the adsorption processes, it is necessary to develop cheaper and easily available adsorbents with high adsorption capacities (8).

Metallic nanoparticles are beginning to receive more attention because of their relatively high chemical activity and specificity of interaction. Control of nanoparticle size, shape, and dispersity is the key to selective and enhanced activity (9).

Iron-based bimetallic nanoparticles such as Fe-Pd, Fe-Pt, Fe-Ag, and Fe-Ni have been synthesized to improve the performance of the zero valent iron technology for remediation of groundwater contaminants like chlorinated aliphatic, chlorinated aromatics, and chlorinated pesticides. The advantages of bimetallic nanoparticles include high surface area and density of reactive surface sites; catalytic effects, which are effective in hydrodehalogenation reactions (10). Previously, it was observed that the combination of porous materials and metal nanoparticles is one of the interesting areas of interdisciplinary research in water treatments (11-13).

Nickel oxide is an interesting p-type transition element semiconductor that possesses unique catalytic, electric, and magnetic properties that extend its application in many industrial fields (14). Recently, a removal based on nickel oxides has been reported by several groups for the effective removal of dyes. The degradation of azo dye Orange G in aqueous solution onto iron-nickel bimetallic nanoparticles has been reported (15), the results show that the presence of catalytic Ni improved the removal by producing more reducing species on the bimetallic surface. These nanoparticles showed a

significantly long life span with sustained reactivity, making them potential candidates for dye degradation technologies. Chen et al. (16) reported the effective adsorption of Congo red dye on $Co_{0.3}Ni_{0.7}Fe_2O_4$ nanoparticles and found a dominant mechanism of chemisorption on the monolayer maximum adsorption capacity (131.75 mg/g), which is high in comparison with many other adsorbents. Ahmed (15) studied the photodegradation of methylene blue using NiO/TiO_2 nanocomposites and found that the presence of nickel oxide plays a vital role in controlling the physicochemical and optical properties of the samples support the photodegradation of dye.

Trujillo-Reyes et al. (11) reported use of Fe–Ni nanostructures and C/Fe–Ni composites as adsorbents for the removal of indigo carmine dye from aqueous solution and found that Fe–Ni nanostructures adsorption capacity was 977.18 mg/g, followed by C/Fe–Ni 75/25% composite with 654.33 mg/g, and a lowest value, 486.41 mg/g, was obtained for C/Fe–Ni 95/5% composite and the sorption mechanism reported was chemisorption on heterogeneous materials.

The indigo carmine is considered a highly toxic indigoid dye and it can cause skin and eye irritations to human beings. It can also cause permanent injury to cornea and conjunctiva. The consumption of the dye can also prove fatal as it is carcinogenic in nature and can lead to reproductive, developmental, neuro and acute toxicity (17).

The aim of this paper was to evaluate the sorption and/or catalytic properties of the *Schoenoplectus acutus* and Ni nanoscale oxides/*Schoenoplectus acutus* composite to remove indigo carmine from aqueous solution, considering parameters such as contact time, concentration, pH, and column experiments because they provide information about various design parameters necessary at field scale (18).

EXPERIMENTAL METHODS

Adsorbent and Chemicals

Indigo Carmine Dye

Indigo carmine (5, 5-indigosulfonic acid, acid blue 74) was obtained from Sigma-Aldrich®. It has two sulphonate groups, a molar mass of 466.35 g/mol, color index number 73,015, and a maximum light absorption at $\lambda_{max} = 617$ nm.

Preparation of the Adsorbent

Schoenoplectus acutus of brown color was dried, cut in little pieces, washed with distilled water to remove the dust, and finally dried in an oven for 3 days at 60°C, then milled and sieved to a particle size of 40 mesh.

Preparation of Ni Nanoscale Oxides/Schoenoplectus acutus Composite

The preparation of the composite was in situ, a 1×10^{-2} M nickel sulfate solution was left in contact with the adsorbent (*Schoenoplectus acutus*), this mixture was shacked at 300 rpm

for 10 minutes, then pH was adjusted to 7.0 by adding a NaOH solution. Finally 100 mL of a $NaBH_4$ solution was added to reduce the Ni, generating a black solid that was filtered, washed with distilled water to remove soluble salts, and then with acetone to remove the water.

Characterization

TEM Observations

Dried Ni nanoscale oxides/Schoenoplectus acutus composite was suspended in 2-propanol using an ultrasonic instrument. TEM samples were prepared by placing a drop of the alcoholic suspension on carbon-coated copper grids. TEM observations were performed on a transmission electron microscope JEOL-2010, operated at an accelerating voltage of 200 kV equipped with a LaB_6 filament.

X-Ray Diffraction

X-ray powder diffraction (XRD) patterns were collected on Bruker X-ray diffractometer model D-8 Advance, equipped with Linxeye detector and source of Cu K_α radiation ($\lambda = 0.1544$ nm).

SEM/EDS Observations

SEM observations were performed by using a JEOL 5900 at 20KV. Microanalyses were done with an EDS (Energy X-Ray Dispersive Spectroscopy) system.

Brunauer-Emmett-Teller Analysis

Brunauer-Emmett-Teller (BET) surface areas were determined by standard multipoint techniques of nitrogen adsorption, using a BELSORP-max instrument. Samples were heated at 200°C for 1 h before specific surface areas were measured.

Sorption Experiments

Batch adsorption experiments were performed in duplicate using a rotating system set at 25 rpm, 10 mL of an indigo carmine solution was added to 10 mg of each adsorbent material (*Schoenoplectus acutus* or Ni nanoscale oxides/*Schoenoplectus acutus* composite), pH was measured before and after the experiments which were performed at room temperature. For kinetics studies, each mixture was in contact during 1, 5, 15, 30, 60, 120, 180, 300, 420, and 600 min with a 100 mg/L indigo carmine solution; isotherms were carried out using 50, 100, 300, 400, 500, 700, 900, and 1,000 mg/L of dye solutions stirring for 180 minutes using Ni nanoscale oxides/*Schoenoplectus acutus* composite. Also, indigo carmine solutions at different pH values (1, 3, 5, 7, 9, 11, and 13) were tested. Each mixture was vacuum filtrated, and dye concentrations were determined in the liquid phases at $\lambda = 617$ nm using a PerkinElmer Lambda 25 UV/Vis spectrophotometer. All experiments were done in duplicate.

The amount of indigo carmine dye onto the corresponding material, q_e (mg/g) was calculated by a mass balance

relationship: $q_e = (C_0–C_e)$ V/W; where C_o (mg/L) and C_e (mg/L) are the initial and the equilibrium liquid-phase concentration of the dye, respectively, V (L) the volume of the solution, and W (g) the weight of the corresponding material.

Fixed Bed Experiments

The fixed-bed column experiments were conducted with a bed height of 2.5 cm in a glass column of 1.0 cm internal diameter. The weight of adsorbent was 0.318 g of Ni nanoscale oxides/*Schoenoplectus acutus* composite, the bed volume was 1.96 cm³. Glass wool was put in the bottom of the column to support the adsorbent.

The column was fed with a solution of 100 mg/L of indigo carmine at a constant volumetric flow rate of 1 mL/min and pH 6.0 in down-flow mode. This volumetric flow rate was calculated according to Tchobanoglous et al. (19). Liquid samples were withdrawn at different intervals of time until the effluent concentration was equal to the influent concentration.

RESULTS AND DISCUSSION

Materials

Ni nanoscale oxides/*Schoenoplectus acutus* composite was obtained efficiently by the method of chemical reduction and it was characterized by using TEM, XRD; this composite and the biosorbent were characterized by SEM/EDS and BET.

Characterization
Transmission Electron Microscopy

TEM images of Ni nanoscale oxides are shown in Fig. 1. It can be observed that the metallic oxides have average sizes of 15 nm, and they do not present a defined structure but aggregates of nanoparticles are observed. Figure 1a shows a 100 nm scale and Fig. 1b shows 50 nm; thus a more defined structure and size of the Ni oxides can be observed.
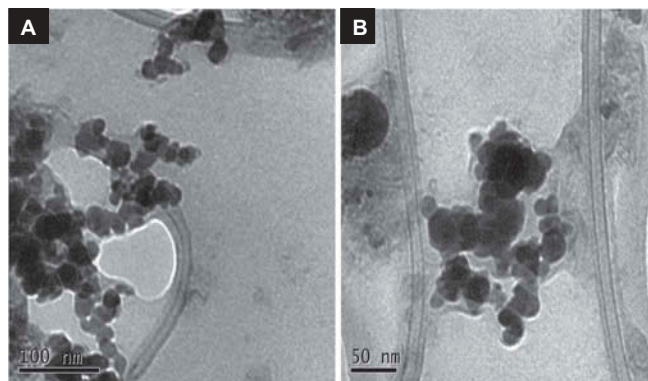

FIG. 1.   Transmission electron microscopy (TEM) images of Ni nanoscale oxides (A and B show 100 and 50 nm scale respectively).

X-Ray Diffraction

The X-ray diffraction patterns of *Schoenoplectus acutus* and Ni nanoscale oxides/*Schoenoplectus acutus* composite have very low crystallinity; the diffractograms do not show well defined diffractions peaks. The diffraction peaks observed for the composite corresponded to nickel, bunsenite, nickel hydroxide hydrate, and nullaginite according to JCPDS cards numbers 451027, 471049, 220444, and 350501, respectively.

Scanning Electron Microscopy

Figure 2a shows the SEM image of *Schoenoplectus acutus* material. It can be appreciated that this material has a block well defined structure. Additionally, after being in contact with indigo carmine solution, the surface was similar as shown in Fig. 2b.

Figure 2c shows the Ni nanoscale oxides/*Schoenoplectus acutus* composite, it is observed that the composite has also a block structure with brilliant small spots which could be the Ni nanoparticles onto the surface of the biosorbent. Figure 2d shows the SEM image of the composite after being in contact with the indigo carmine dye, which does not show any change in the morphology of the material.

Table 1 shows EDS analysis of the *Schoenoplectus acutus* and the *Ni nanoscale oxides/Schoenoplectus acutus composite* before and after they were in contact with indigo carmine.

EDS analysis indicates a simple composition for both materials. *Schoenoplectus acutus* contains carbon and oxygen; after the material was in contact with the dye, calcium appeared in the sample in less than one percent and this might be from the aqueous solutions. *Ni nanoscale oxides/Schoenoplectus acutus* contains carbon, oxygen, and nickel; after indigo carmine was in contact with the material, sulfur appeared in less than one percent. It is important to note that the dye molecule has sulfonic groups and its presence may indicate that the dye adsorption on the composite occurred.

BET Analysis

The dye adsorption capacities depend on the characteristics of each individual adsorbent, the extent of surface modification and the initial concentration of adsorbate, among others (20). The BET surface areas for *Schoenoplectus acutus* and Ni nanoscale oxides/*Schoenoplectus acutus* composite were 0.140 and 13.62 m²/g, respectively. Then sorption capacity increased when Ni nanoparticles were supported on the biosorbent.

Adsorption Kinetic Behavior

The kinetic parameters are calculated by fitting the experimental results to mathematical models reported in the literature; the most utilized models are the pseudo first order or Lagrergren, the second order or Elovich, and the pseudo second order or Ho and McKay (3) which are described below.
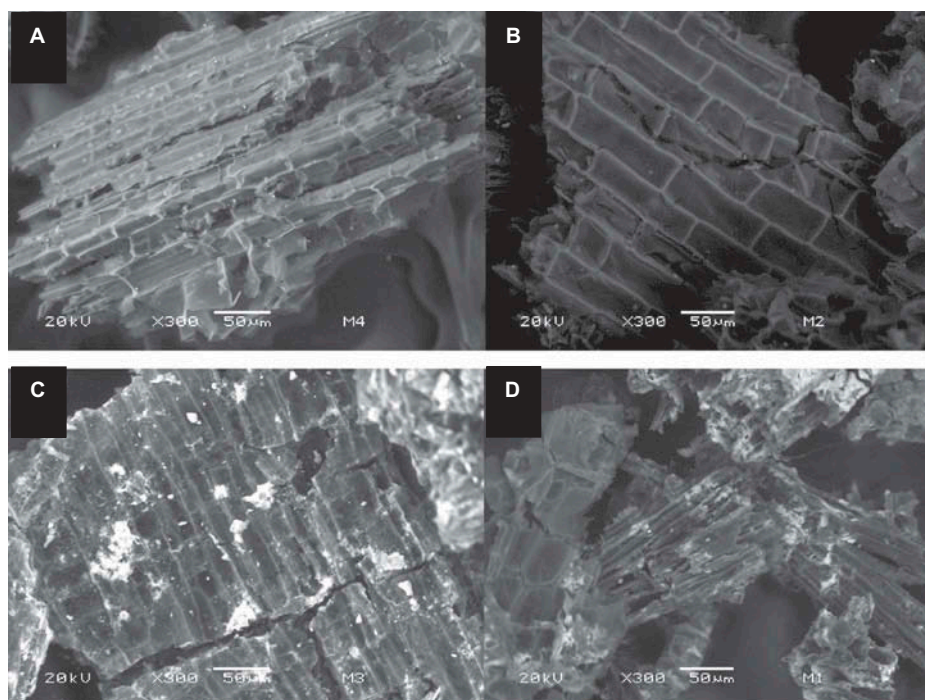
FIG. 2. Scanning electron microscopy (SEM) images of (A) *Schoenoplectus acutus* before indigo carmine contact, (B) after indigo carmine contact, (C) Ni nanoscale oxides/*Schoenoplectus acutus* composite before IC contact and (D) after indigo carmine contact.

TABLE 1
Elemental analysis of Ni nanoscale oxides/*Schoenoplectus acutus* composite and *Schoenoplectus acutus*. before and after being in contact with indigo carmine.

	Before sorption		After sorption	
Element	Weight percent *Schoenoplectus acutus*	Weight percent Ni/ *Schoenoplectus acutus*	Weight percent *Schoenoplectus acutus*	Weight percent Ni/ *Schoenoplectus acutus*
C	59.20 ± 0.69	52.38 ± 5.28	62.15 ± 0.12	42.11 ± 4.54
O	40.79 ± 0.69	28.88 ± 8.03	36.96 ± 0.28	16.83 ± 5.35
Ni	——	18.73 ± 3.52	——	40.65 ± 8.26
Ca	——	——	0.88 ± 0.11	——
S	——	——	——	0.41 ± 0.13

The experimental results were adjusted to these models with the help of STATISTICA 6.0 software.

In the pseudo first order model (Lagrergren), the sorption velocity is proportional to the concentration of the adsorbate. It is used for adsorbent materials with a homogeneous surface and physical sorption (21). The adsorption velocity can be expressed as: $q_t = q_e (1-e^{\wedge}(-K_L t))$; where q_e (mg/g) and q_t (mg/g) are the dye amount adsorbed in the equilibrium and in time t, respectively, and K_L is the Lagregren constant (h^{-1}). Figure 3 shows the kinetic sorption behavior of indigo carmine dye from aqueous solution using *Schoenoplectus acutus* and Ni nanoscale oxides/*Schoenoplectus acutus* composite,
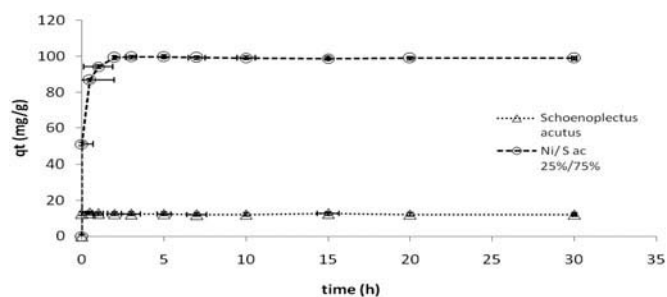

FIG. 3. Sorption kinetics of indigo carmine by *Schoenoplectus acutus* and Ni nanoscale oxides/*Schoenoplectus acutus* composite.

the equilibrium was reached in less than 1 hour for *Schoeno-plectus acutus* and less than 5 hours for Ni nanoscale oxides/*Schoenoplectus acutus* composite, the results could be fitted to this model, the indigo carmine amount adsorbed at the equilibrium was almost 8 times higher for the composite (97.7 mg/g) than for *Schoenoplectus acutus* (12.4 mg/g). The Lagergren constant was higher for *Schoenoplectus acutus* (1789 h^{-1}) than for Ni nanoscale oxides/*Schoenoplectus acutus* composite (74.2 h^{-1}) with r^2 values higher than 0.99 for both cases.

The second order model (Elovich) indicates chemisorption processes and that the adsorbent is heterogeneous and hence exhibit different energies of activation (22). The Elovich model includes diffusion in the solution and in the surface, activation, and deactivation of the catalytic surfaces and it is represented as: $q_t = 1/b \ln(ab) + 1/b \ln t$; where q_t is the amount of indigo carmine adsorbed in a time t, "a" is the sorption constant (mg/g), and "b" is the desorption constant (mg/g). The "a" values determined for *Schoenoplectus acutus* (22188 mg/g) and Ni nanoscale oxides/Schoenoplectus acutus composite (18683 mg/g) were much higher than the values determined for "b" for *Schoenoplectus acutus* (1.8 mg/g) and Ni nanoscale oxides/*Schoenoplectus acutus* composite (0.2 mg/g), this behavior indicates a high affinity of the adsorbents for the adsorbate and probably the adsorption mechanism is chemisorption; r^2 values were 0.929 and 0.981 for *Schoenoplectus acutus* and Ni nanoscale oxides/*Schoenoplectus acutus* composite, respectively.

The pseudo second order model was developed by Ho and McKay (3). A lot of research has reported a good fit of the experimental data to this model and it indicates that a chemical adsorption mechanism can take place, it is represented as: $q_t = (Kq_e^2 t)/(1+Kq_e t)$; where q_e (mg/g) and q_t (mg/g) are the dye amount adsorbed in the equilibrium and in time t respectively, K (g/mg h) is the adsorption kinetic constant. The indigo carmine amount adsorbed at the equilibrium was higher for the composite (97.9 mg/g) than for *Schoenoplectus acutus* (12.4 mg/g), but the K constant was higher for *Schoenoplectus acutus* (34946 g/mg h) than for Ni nanoscale oxides/*Schoenoplectus acutus* composite (1.1 g/mg h) with r^2 values over 0.99 for both materials.

Although, the experimental data could be fitted to these three models with good correlation values, this last model is probably the most appropriate one to be applied to this sorption system because according to the characterization of the adsorbents they are heterogeneous materials, and in previous works using Fe-Cu and Fe-Ni nanoscale oxides and some dyes (11-13), it was observed that this last model was best fitted to the results; therefore, a chemisorption mechanism probably occurs on heterogeneous materials. Since the adsorption capacity for Ni nanoscale oxides/*Schoenoplectus acutus* composite was almost 8 times higher than the sorption capacity for *Schoenoplectus acutus*, and the isotherm and the column studies were performed only with the composite.

Isotherm Models

Irving Langmuir developed a simple isotherm model that can be applied to the solid-liquid and solid-gas interfaces (23). The solid surface contains a determined number of adsorption sites. At equilibrium, the adsorption and desorption velocities are the same. Adsorbate molecules form a monolayer in the surface of the adsorbent. Then all adsorption sites are equivalent and the surface is uniform. The equation is generally used for chemisorption and can be expressed as: $q_e = (q_0 b C_e)/(1+bC_e)$; where q_0 (mg/g) is the maximum adsorption capacity, b is a constant related to the energy or net enthalpy of adsorption, and C_e is the indigo carmine concentration in the solution at equilibrium (mg/L). The results of the isotherm for Ni nanoscale oxides/*Schoenoplectus acutus* composite could be fitted to this model and the parameters obtained were $q_0 = 860.2$ mg/g, b = 0.0057, and $r^2 = 0.948$. Although the results could be fitted and q_0 value calculated, this is not the best model to be used with this adsorbent, because the Langmuir model is for homogeneous adsorbents and the material most probably is a heterogeneous adsorbent according to its characterization.

The Freundlich isotherm model is an exponential equation; it assumes that when the adsorbate concentration in the solution increases, the adsorbate concentration in the adsorbent surface also increases (24-25). It is used in materials with heterogeneous surfaces where the different sorption energies are because of the variations in the heat of adsorption (21, 23) involving physical sorption. The Freundlich isotherm model is represented as: $q_e = K_F C_e^{1/n}$; where q_e (mg/g) is the amount of dye adsorbed, K_F is the equilibrium Freundlich constant, C_e is the concentration of the dyestuff in the solution at equilibrium (mg/L), n is the adsorption constant at equilibrium whose reciprocal (1/n) is a measure of the heterogeneity of the adsorption surface, also indicates the adsorption intensity, if $1/n < 1$ the adsorption is favorable and if $1/n > 1$ the adsorption is unfavorable. Figure 4 shows the experimental data fitted to this
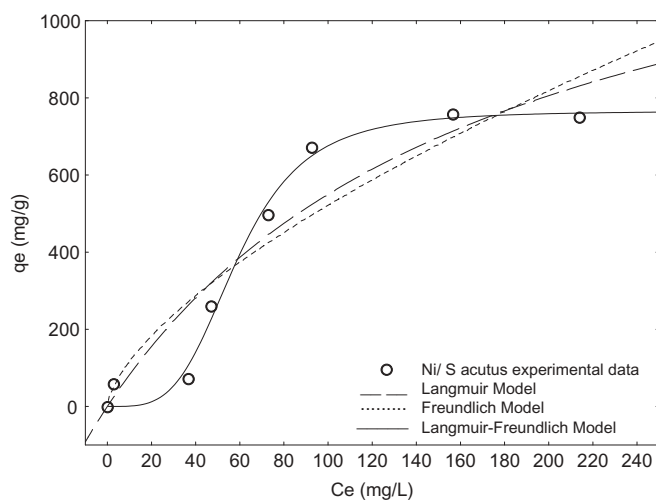

FIG. 4. Isotherm models applied to the sorption of indigo carmine by Ni nanoscale oxides/*Schoenoplectus acutus* composite.

model, the parameters obtained for Ni nanoscale oxides/Schoenoplectus acutus composite were $K_F = 26.043$ g mg$^{1/n-1}$ and n = 1.53 with $r^2 = 0.934$. Values of 1/n less than unity imply a heterogeneous surface structure with minimum interaction between adsorbed atoms [26]; also, the value of 1/n (0.65) indicates that the adsorption is favorable with this composite.

The Langmuir-Freundlich isotherm model is a combination of Langmuir and Freundlich models which indicates that involves an adsorption by combined mechanisms onto heterogeneous materials. This model is expressed as: $q_e = (KC_e^{1/n})/(1 + bC_e^{1/n})$; where, q_e is the amount of dye adsorbed in mg/g, C_e is the equilibrium concentration of dye in solution (mg/L), K, b and 1/n are empirical constants. The parameters obtained for Ni nanoscale oxides/*Schoenoplectus acutus* composite were K = 9.08 g mg$^{1/n-1}$ and n = 0.965 with $r^2 = 0.971$; this model gave the highest r^2 value and it indicates that the sorption takes place by combined mechanisms on heterogeneous materials. The adjustment of the experimental data is presented in Fig. 4.

Effect of pH

pH is an important parameter due to the ionization of surface functional groups and the composition of solutions. The adsorption of indigo carmine by Ni nanoscale oxides/*Schoenoplectus acutus* composite at different pH values showed that the adsorption capacities are not affected by pH in the range from 3 to 9 and then decrease sharply (Fig. 5).

Since the dye has sulfuric groups in the chemical structure, which is negatively charged, possibly the acidic solution favors adsorption of dye onto catalyst surface, which acquires positive charge in acidic solution [27]. According to the pK values reported for this dye which are higher than 11 and Fig. 5, it is possible that the neutral species of the dye are preferable adsorbed by the Ni nanoscale oxides/*Schoenoplectus acutus* composite.

Fixed Bed Experiments

The breakthrough curve was obtained by plotting C_e/C_o (effluent concentration/influent concentration) vs. time. The breakthrough time (t_b) chosen was the time where dye
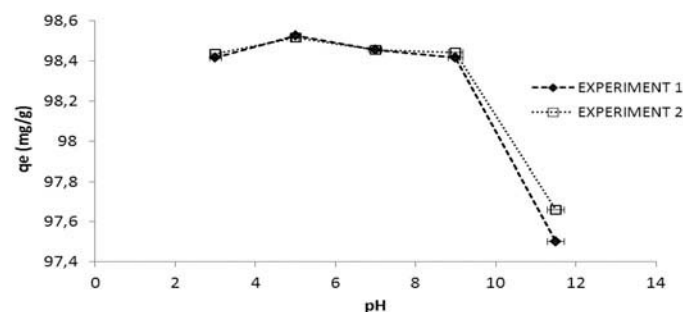

FIG. 5.   pH effect on the adsorption of indigo carmine by Ni nanoscale oxides/*Schoenoplectus acutus* composite.

concentration in the effluent was 10 mg/L, the bed saturation time (t_{sat}) was chosen to be the time where dye concentration in the effluent reached 90% of the initial dye concentration. The maximum column capacity, q_{total} (mg), for a given feed concentration and flow rate [28] is equal to the area under the plot of the adsorbed indigo carmine concentration, C_{ad} ($C_{ad} = C_e - C_o$) (mg/L) vs. effluent time (t, min) and it is calculated from Eq. (1):

$$q_{total} = \frac{QA}{1000} = \frac{Q}{1000} \int_{t=0}^{t=t_{total}} C_{ad} dt \tag{1}$$

where t_{total}, Q and A are the total flow time (min), volumetric flow rate (mL/min) and the area under the breakthrough curve, respectively. The equilibrium uptake ($q_{eq(exp)}$) is calculated as follows:

$$q_{eq(exp)} = \frac{q_{total}}{m} \tag{2}$$

where m is the total dry weight of Ni nanoscale oxides/*Schoenoplectus acutus* composite in column (g). The total amount of indigo carmine sent to the column (W_{total}) is calculated from the following equation:

$$W_{total} = \frac{C_0 Q t_{total}}{1000} \tag{3}$$

Total removal percent of indigo carmine is the ratio of the maximum capacity of the column (q_{total}) to the total amount of indigo carmine sent to column (W_{total}).

$$Y = \left(\frac{q_{total}}{W_{total}}\right) \times 100 \tag{4}$$

The parameters such as q_{total}, q_{eq}, W_{total}, and Y (%) were evaluated for the removal of indigo carmine using Ni nanoscale oxides/*Schoenoplectus acutus* composite in the fixed-bed adsorption column. The $q_{total} = 48.42$ mg, $W_{total} = 93.8$ mg, and Y = 51.6%. The amount adsorbed of indigo carmine per unit mass of Ni nanoscale oxides/*Schoenoplectus acutus* composite ($q_{eq(exp)} = 76.13$ mg/g) estimated using the fixed-bed column is 11 times lower than that predicted by using Langmuir model (860.2 mg/g), these results are reasonable because the adsorption equilibrium in fixed bed systems is not reached as it is in batch systems.

The total removal percent of indigo carmine was 51.62% for Ni nanoscale oxides/Schoenoplectus acutus composite, Mittal et al. [17] reported saturation percentages at the breakpoint for indigo carmine–bottom ash and indigo carmine de-oiled soya columns of 42.76% and 43.99%, respectively.

Three models were used to predict the dynamic behavior of the column: Bohart-Adams, Thomas, and Yoon-Nelson models, the experimental results were adjusted to these models with the help of STATISTICA 6.0 software. Figure 6 shows the
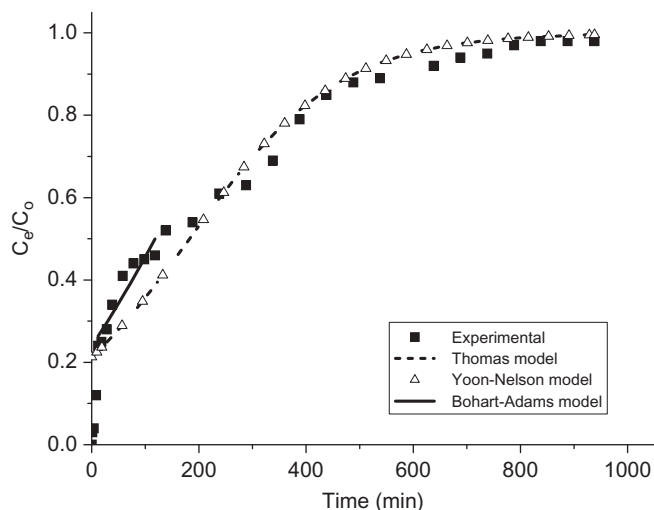
FIG. 6. Breakthrough curves of indigo carmine dye by Ni/*Schoenoplectus acutus* composite and adjustments to Thomas, Yoon-Nelson and Bohart-Adams models.

adjustments of the experimental results to these models and Table 2 summarize the parameters calculated for the adsorption of indigo carmine by Ni nanoscale oxides/Schoenoplectus acutus composite.

The Bohart-Adams model is used for the description of kinetic data until 50% adsorption was reached, the Thomas and Yoon-Nelson models were also applied to the adsorption kinetics data up to saturation.

The treated aqueous solution volume at breakthrough region was 8 mL, the bed volumes at saturation were 325 BV and the aqueous solution volume treated was 638 mL. Those results indicate that after 8 min of service time, the breakthrough occurs.

The breakthrough regions could be reached in longer times, if the residence time is increased by using a larger bed length or a lower feed flow rate to allow the solute to reach the adsorption sites. However, in the case of industrial application, long residence time is not favorable due to economic constraints (29).

The Bohart-Adams model is used to describe the initial part of a breakthrough curve. The expression is the following (30):

$$\frac{C}{C_0} = \exp\left(k_{AB}C_0t - k_{AB}N_0\frac{Z}{F}\right) \quad (5)$$

where k_{AB} is the kinetic constant (Lmg^{-1} min^{-1}), F is the linear flow rate (cm min^{-1}), Z is the bed depth of column (cm), and N_o is adsorption capacity (mg L^{-1}). The experimental data were fitted to this model, the r^2 parameter (0.858) indicates the correlation between the experimental points and predicted values, suggesting that Bohart-Adams model may be valid for the adsorption processes where C_e/C_o region was up to 0.5 at all operating conditions. Although the Bohart-Adams model provides a simple and comprehensive approach to evaluate the adsorption column process, its validity is limited to the range of conditions used in the column (30).

The Thomas model assumes a constant separation factor but it is applicable to either favorable or unfavorable isotherms (31). Adsorption is usually not limited by chemical reaction kinetics but it is often controlled by mass transfer. The expression of Thomas model for an adsorption column is given as follows:

$$\frac{C}{C_o} = \frac{1}{1 + \exp(K_{Th}q_om/Q - K_{Th}C_ot)} \quad (6)$$

where K_{Th} is the Thomas rate constant (L min^{-1}.mg^{-1}), q_o is the adsorption capacity of adsorbent (mg g^{-1}), Q is the volumetric flow rate (L min^{-1}), and m is the mass of the adsorbent (g).

Han et al. (30) found that factors such as pH, existed salt, flow rate, influent concentration of dye, and bed depth could influence the performance of breakthrough curves, so the variation in the slope of the breakthrough curve may be explained on the basis of mass transfer. Table 2 shows that the model gave a good fit of the experimental data with a correlation coefficient of 0.930.

Finally, the Yoon-Nelson model is based on the assumption that the rate of decrease in the probability of adsorption for each adsorbate molecule is proportional to the probability of adsorbate adsorption and the probability of adsorbate breakthrough on the adsorbent (31-32). The Yoon and Nelson equation regarding a single component system is expressed as (28):

$$\frac{C}{C_o} = \frac{\exp(K_{YN}t - \tau K_{YN})}{1 + \exp(K_{YN}t - \tau K_{YN})} \quad (7)$$

where K_{YN} is the rate constant (min^{-1}); τ, the time required for 50% adsorbate breakthrough (min). Due to the symmetrical nature of the breakthrough curve, the amounts of dye adsorbed

TABLE 2
Bohart-Adams, Thomas and Yoon-Nelson parameters for Ni nanoscale oxides /*Schoenoplectus acutus* composite.

			Yoon-Nelson model				Bohart-Adams model		
q_o (mg/g)	$K_{Th} \times 10^{-5}$ (L/mg min)	r^2	q_o (mg/g)	K_{YN} (L/min)	τ (min)	r^2	N_o (mg/L)	$k_{AB} \times 10^{-5}$ (L/mg min)	r^2
57.39	7.15	0.930	57.38	0.0071	182.52	0.930	19734.52	1.95	0.858

by the adsorbents are one half of the total indigo carmine entering the adsorption column within the 2τ period. Hence the following equation can be written (31):

$$q_0 = \frac{1}{2}\frac{C_0 Q(2\tau)}{m} = \frac{C_0 Q\tau}{m} \qquad (8)$$

This equation also permits the determination of the adsorption capacity of the column (q_o) as a function of initial dye concentration (C_o), flow rate (Q), mass quantity in the column (m), and 50% breakthrough time (τ). The 50% breakthrough time (τ) obtained was 182.52 minutes corresponding at experimental values (168 min); however, the breakthrough curve does not present a symmetrical nature at second region; therefore $2(\tau)$ value from the calculation were significantly different compared with experimental results, it can be concluded that the experimental data could be fitted to Yoon-Nelson model, especially the data from the first region. According to Fig. 6, it is observed that the adsorption capacities and r^2 parameters calculated by the Thomas and Yoon-Nelson models are similar.

Comparisons of Ni Nanoscale Oxides/*Schoenoplectus acutus* Composite with Other Materials for the Adsorption of Indigo Carmine

Table 3 shows the adsorption capacities for indigo carmine using different adsorbents; it is difficult to compare the results of this work with those from the literature because the adsorption capacities were determined in different experimental conditions, depending on the dye concentration, chemical composition of adsorbent, etc. The adsorbent used in this study shows a much higher adsorption capacity in comparison with other adsorbent materials reported in the literature. As can be observed in Table 3, nanocomposite hydrogels shows a sorption capacity for indigo carmine of 370.37 mg/g and the capacity found in this work for Ni nanoscale oxides/*Schoenoplectus acutus* composite was 860.2 mg/g, these results show

TABLE 3
Comparisons of of Ni nanoscale oxides/*Schoenoplectus acutus* composite with other materials for the adsorption of indigo carmine.

Adsorbent	q_{max} (mg/g) batch	Reference
Brazil nut shell	1.09	(33)
Rice husk ash	29.27	(34)
Zeolitic material	32.83	(35)
Activated sewage sludge	60.04	(36)
Pyrolysis of sewage sludge	92.83	(35)
Nanocomposite hydrogels	370.37	(37)
Ni nanoscale oxides/ *Schoenoplectus acutus* composite	860.2	This work

that this last material is a promising adsorbent for the removal of dyes.

CONCLUSIONS

Removal of dye contaminants from wastewaters using metal nanoparticles supported on a low-cost adsorbent was investigated. Ni nanoscale oxides/*Schoenoplectus acutus* composite was obtained efficiently by the chemical method of salts reduction. The adsorbent was characterized and Ni was found in the composite. Ni nanoscale oxides/*Schoenoplectus acutus* composite showed a surface area relatively low, this factor did not affected the sorption of dye on the material. Pseudo second order and Langmuir-Freundlich models provide the best correlation of the experimental data for the Ni nanoscale oxides/*Schoenoplectus acutus* composite, indicating chemisorption processes onto a heterogeneous material. In addition, this material provides high adsorption capacity according to the Langmuir model and the removal of the dye is not affected by the pH in the range between 3 and 9. The adsorption capacity of Ni nanoscale oxides/Schoenoplectus acutus composite (76.13 mg/g) estimated using a fixed-bed column was 11 times lower than that predicted by using Langmuir model (860.2 mg/g). Fixed bed experiments results could be fitted to Thomas, Yoon-Nelson, and Bohart-Adams models. It is important to note that Ni nanoscale oxides/Schoenoplectus acutus composite is a promising adsorbent for the removal of dyes from wastewater because it showed a high capacity in comparison with many other adsorbents.

REFERENCES

1. Bhatnagar, A. M.; Jain, A. K. (2005) A comparative adsorption study with different industrial wastes as adsorbents for the removal of cationic dyes from water. J. Colloid Interface Sci., 281: 49–55.
2. Crini, G.; Badot, P. M. (2008) Application of chitosan, a natural aminopolysaccharide, for dye removal from aqueous solutions by adsorption processes using batch studies: A review of recent literature. Prog. Polym. Sci., 33: 399–447.
3. Ho, Y. S.; McKay, G. (1998) Sorption of dye from aqueous solution by peat. Chem. Eng. J., 70: 115–124.
4. McKay, G.; Poots, V. J. P. (1980) Kinetics and diffusion processes in color removal from effluent using wood as an adsorbent. J. Chem. Technol. Biotechnol., 30: 279–292.
5. McKay, G. (1984) Analytical solution using a pore diffusion model for a pseudoirreversible isotherm for the adsorption of basic dye on silica. AIChE J., 30: 692–697.
6. Dogan, M.; Alkan, M.; Onganer, Y. (2000) Adsorption of methylene blue on perlite from aqueous solutions. Water, Air, Soil Poll., 120: 229- 248.
7. Namasivayam, C.; Kavitha, D. (2003) Adsorptive removal of 2-chlorophenol by low-cost coir pith carbon. J. Hazard. Mater., B98: 257–274.
8. Dogan, K. (2007) Modeling the mechanism, equilibrium and kinetics for the adsorption of acid orange 8 onto surfactant-modified clinoptilolita: The application of nonlinear regression analysis. Dyes Pigments, 74: 659–664.

9. White, R. J.; Luque, R.; Budarin, V. L.; Clark, J. H.; Macquarrie, D. J. (2008) Supported metal nanoparticles on porous materials: Methods and applications. Chem. Soc. Rev., 38: 481–494.

10. Bokare, A. D.; Chikate, R. C.; Rode, C. V.; Paknikar, K. M. (2007) Effect of surface chemistry of Fe-Ni nanoparticles on mechanistic pathways of azo dye degradation. Environ. Sci. Technol., 41: 7437–7443.

11. Trujillo-Reyes, J.; Solache-Ríos, M.; Vilchis-Nestor, A.; Sánchez-Mendieta, V.; Colín-Cruz, A. (2012a) Fe–Ni nanostructures and C/Fe–Ni composites as adsorbents for the removal of a textile dye from aqueous solution. Water, Air and Soil Poll., 223: 1331–1341.

12. Trujillo-Reyes, J.; Sánchez-Mendieta, V.; Solache-Ríos, M.; Colín-Cruz, A. (2012b) Removal of remazol yellow from aqueous solution using Fe–Cu and Fe–Ni nanoscale oxides and their carbonaceous composites. Environ. Technol., 33: 545–554.

13. Trujillo-Reyes, J.; Sánchez-Mendieta, V.; Colín-Cruz, A.; Morales-Luckie, R. (2010) Removal of Indigo Blue in aqueous solution using Fe/Cu nanoparticles and C/Fe-Cu nanoalloy composites. Water, Air and Soil Poll., 207: 307–317.

14. Ahmed, M. A. (2012) Synthesis and structural features of mesoporous NiO/TiO2 nanocomposites prepared by sol–gel method for photodegradation of methylene blue dye. J. Photochem. Photobiol. A: Chem. 238: 63–70.

15. Bokare, A. D.; Chikate, R. C.; Rode, Ch. V.; Paknikar, K. M. (2008) Iron-nickel bimetallic nanoparticles for reductive degradation of azo dye orange G in aqueous solution. Applied Catalysis B: Environmental. 79: 270–278.

16. Chen, R.; Wang, W.; Zhao, X.; Zhang, Y.; Wu, S.; Li, F. (2014) Rapid hydrothermal synthesis of magnetic $CoxNi1\_xFe2O4$ nanoparticles and their application on removal of congo red. Chem. Eng. J. 242: 226–233.

17. Mittal, A.; Mittal, J.; Kurup, L. (2006) Batch and bulk removal of hazardous dye, indigo carmine from wastewater through adsorption. J. Hazard. Mater., B137: 591–602.

18. Jang, A.; Lee, S. W.; Seo, Y.; Kim, K. W.; Kim, I. S.; Bishop, P. L. (2007) Application of mulch for treating metals in urban runoff: batch and column test. Water Sci. Technol., 55: 96–103.

19. Tchobanoglous, G.; Burton, F. L.; Stensel, H. D. (2003) Wastewater Engineering: Treatment and Reuse, McGraw-Hill: New York.

20. Demirbas, A. (2009) Agricultural based activated carbons for the removal of dyes from aqueous solutions: A review. J. Hazard. Mater., 167 (1–3): 1–9.

21. Mathialagan, T.; Viraraghavan, T. (2003) Adsorption of cadmium from aqueous solutions by vermiculite. Sep. Sci. Technol., 38: 57–76.

22. Demirbas, E.; Kobya, M.; Senturk, E.; Ozkan, T. (2004) Adsorption kinetics for the removal of chromium (VI) from aqueous solutions on the activated carbons prepared from agricultural wastes. Water SA, 30: 533–540.

23. Slejko, F. L. (1985) Adsorption Technology: A Step By Step Approach to Process Evaluation and Application; Marcel Dekker: New York.

24. Allen, S. J.; McKay, G.; Porter, J. F. (2004) Adsorption isotherm models for basic dye adsorption by peat in single and binary component systems. J. Colloid Interface Sci., 280: 322–333.

25. Freundlich, H. M. F. (1906) Over the adsorption in solution. J. Phys. Chem., 57: 370–485.

26. Abou-Mesalam, M. M. (2004) Applications of inorganic ion exchangers: II. Adsorption of some heavy metal ions from their aqueous waste solution using synthetic iron III titanate. Adsorption, 10: 87–92.

27. Othman, I.; Mohamed, R. M.; Ibrahim, I. A.; Mohamed, M. M. (2006) Synthesis and modification of ZSM-5 with manganese and lanthanum and their effects on decolorization of indigo carmine dye. Appl. Catal. A, 299: 95–102.

28. Yahaya, N.; Abustan, I.; Latiff, M.; Bello, O.; Ahmad, M. (2011) Fixed-bed column study for Cu (II) removal from aqueous solutions using rice husk based activated carbon. Int. J. Eng. Technol., 11: 248–252.

29. Ahmad, A. L.; Chong, M. F.; Bhatia, S. (2006) Prediction of break-through curves for adsorption of complex organic solutes present in palm oil mill effluent (POME) on granular activated carbon. Ind. Eng. Chem. Res., 45: 6793–6802.

30. Han, R.; Wang, Y.; Yu, W.; Zou, W.; Shi, J.; Liu, H. (2007) Biosorption of methylene blue from aqueous solution by rice husk in a fixed-bed column. J. Hazard. Mater., 141: 713–718.

31. Köse, T. E.; Öztürk, N. (2008) Boron removal from aqueous solutions by ion-exchange resin: column sorption-elution studies. J. Hazard. Mater., 152: 744–749.

32. Hasan, S. H.; Ranjan, D.; Talat, M. (2010) Agro-industrial waste 'wheat bran' for the biosorptive remediation of selenium through continuous up-flow fixed-bed column. J. Hazard. Mater., 181: 1134–1142.

33. Modesto de Oliveira, Brito, S.; Martins, Carvalho, Andrade, H.; Frota, Soares, L.; Pires de Azevedo, R. (2010) Brazil nut shells as a new biosorbent to remove methylene blue and indigo carmine from aqueous solutions. J. Hazard. Mater., 174: 84–92.

34. Lakshmi, U. R.; Srivastava, V. C.; Mall, I. D.; Lataye, D. H. (2009) Rice husk ash as an effective adsorbent: evaluation of adsorptive characteristics for indigo carmine dye. J. Environ. Manage., 90: 710–720.

35. Gutiérrez-Segura, E.; Solache-Rios, M.; Colin-Cruz, A. (2009) Sorption of indigo carmine by a Fe-zeolitic tuff and carbonaceous material from pyrolyzed sewage sludge. J. Hazard. Mater., 170: 1227–1235.

36. Otero, M.; Rozada, F.; Calvo, L. F.; García, A. I.; Morán, A. (2003) Elimination of organic water pollutants using adsorbents obtained from sewage sludges. Dyes and Pigments, 57: 55–65.

37. Dalaran, M.; Emik, S.; Güçlü, G.; İyim, T.B.; Özgümüş, S. (2011) Study on a novel polyampholyte nanocomposite superabsorbent hydrogels: Synthesis, characterization and investigation of removal of indigo carmine from aqueous solution. Desalination, 279: 170–182.